Article:

Qu, Z. orcid.org/0000-0002-6671-2647, Zhou, Y. orcid.org/0000-0003-1506-7964, Kelly, J.R. et al. (3 more authors) (2024) A reconfigurable transmitarray unit cell employing liquid metal. IET Microwaves, Antennas & Propagation, 18 (12). pp. 985-991. ISSN 1751-8725

https://doi.org/10.1049/mia2.12518

Received: 30 April 2024 | Revised: 19 August 2024 | Accepted: 23 September 2024

IET Microwaves, Antennas & Propagation

DOI: 10.1049/mia2.12518

The Institution of Engineering and Technology WILEY

ORIGINAL RESEARCH

A reconfigurable transmitarray unit cell employing liquid metal

Zhishu Qu[1] | Yihua Zhou[2] | James R. Kelly[2] | Zhengpeng Wang[3] | Kenneth Lee Ford[4] | Yue Gao[1]

[1]School of Computer Science, Fudan University, Shanghai, China

[2]Electronic Engineering and Computer Science, Queen Mary University of London, London, UK

[3]Electromagnetic Laboratory, School of Electronic and Information Engineering, Beihang University (BUAA), Beijing, China

[4]Department of Electronic and Electrical Engineering, The University of Sheffield, Sheffield, UK

Correspondence

Yihua Zhou.
Email: yihua.zhou@qmul.ac.uk

Funding information

China Postdoctoral Science Foundation, Grant/Award Number: 2023TQ0076; Engineering and Physical Sciences Research Council, Grant/Award Numbers: EP/P008402/1, EP/P008402/2

Abstract

In this paper, a reconfigurable transmitarray unit cell using liquid metal is presented. It consists of three conducting layers where the geometries of the resonators, on the different layers, differ and consist of an arrow shape together with rotated split rings. The arrow-shaped conducting layer has the capability to convert the polarization of the incoming waves by 90°. The split ring resonators, on the upper and lower conducting layers, have the same dimensions but different orientations (horizontal and vertical polarization). Several fluidic channels are placed beneath/above the conducting layers. The transmission behaviour of the unit cell can be changed by altering the geometrical parameters which is achieved by injecting the liquid metal into the channels. More than 300° phase shift range with a maximum S21 of ~ −1.5 dB at 3.3 GHz is obtained. It exhibits 3 dB of insertion loss over a bandwidth ranging from 3.2 to 3.43 GHz. It is the first time that a transmitarray unit cell, reconfigured employing liquid metal, provides a combination of low insertion loss and large phase shift range. The proposed prototype was fabricated and measured within an open-ended waveguide and the measured results agree well with the simulations and verify the effectiveness of the design. The reconfigurable transmitarray unit cell can be used to design beam-scanning arrays, as well as for applications in wireless communications.

KEYWORDS

antenna arrays, metamaterial antennas, microwave antenna arrays, phase shifters, transmitting antennas

1 | INTRODUCTION

Transmitarray antennas are gaining an increasing interest for use within satellite internet and radar applications due to their advantages of low profile, high gain, and beam steering capabilities. Transmitarray antennas convert the spherical phase front from the feed to a planar wavefront which has higher directivity. This is achieved by tuning the transmission phase of individually unit cell locating on the transmitting surface at a specific value. Dynamic reconfiguration of the transmission phase of each unit cell enables beam steering. Commonly, one of the following devices is used to reconfigure the phase of a transmitarray unit cell: 1) varactor diodes [1, 2]; 2) PIN diodes [3, 4]; or 3) microelectromechanical system switches [5]. These devices have the advantages of fast response time and programmable features, which could be automatically controlled by a computer program [6, 7]. However, PIN diodes exhibit intermodulation distortion and significant power loss which will lower the radiation efficiency, especially in high frequency band. Compared to existing approaches for reconfiguring the phase, fluidic material is a promising approach which yields lower power losses and is expected to allow greater power handing capability together with enhanced tuning range. In particular, liquid metal, based on gallium alloys, has attracted more attention recently due to the above advantages together with its low toxicity, high conductivity, and good flexibility.

Many reconfigurable antennas employing liquid metal have recently been published [8–11], including: pattern reconfiguration, frequency reconfiguration, and polarization reconfiguration. However, most of above designs are focused on single antennas, only a few designs employing liquid metal have successfully achieved phase shifting or the unit cells applied in arrays [12–14]. Ref. [12] presents a fluidically tuneable transmitarray unit cell which provides a 360°phase shifting range. The unit cell is based on a fifth-order bandpass structure. By moving droplets of liquid metal through a small distance, the frequency response, and thus the transmission phase of the unit cell, can be continuously tuned. In this way, a 360° phase shift range can be achieved with 1 dB of insertion loss. Their work demonstrates the potential for employing liquid metal in transmitarray unit cells. However, the fifth-order bandpass response consisting of nine metal layers and eight dielectric substrates increases the difficulties involved in fabrication and the actuation (or movement) of liquid metal. Refs. [13, 14] demonstrate the possibility of using liquid metal on the split ring resonators (SRR) to achieve phase shifting. However, they have the disadvantages of narrow phase shifting range or high insertion loss.

This paper presents a reconfigurable transmitarray unit cell employing liquid metal with simplified structure. The proposed unit cell has a low profile with only three conducting layers. By actuating (i.e. moving) the liquid metal into/out of the channels, the conductive regions can be changed. Using this approach, the transmission phase of the unit cell can be switched in several states. The paper is organized as follows: Section 2 gives the design concept and numerical results. Section 3 illustrates the fabrication processing and the measured results. Conclusion is given in Section 4.

2 | UNIT CELL DESIGN AND NUMERICAL RESULTS

In this section, the design process, parametric study and numerical results of the proposed unit cell are introduced.

2.1 | Pro-design

Split Ring Resonator (SRR) is commonly used within microwave circuits and antennas. Recently, it was demonstrated that an SRR tuneable filter incorporating liquid metal can be tuned by adjusting the size and position of the air gap within the section of liquid metal [14]. This is because a single SRR can be modelled using a lumped element LC circuit, as shown in Figure 1. The resonant frequency (ω_0) of the SRR is given as follows:

$$\omega_0 = \sqrt{\frac{1}{LC}} \tag{1}$$

where the capacitance (C) is associated with the gap and the inductance (L) is related to the conducting track. However, conventional SRR structure cannot provide the phase shifting range needed by the transmitarray unit cell. Adding new resonator can help expand the phase shifting range. Thus, an arrow-shaped resonator in the middle layer is designed.

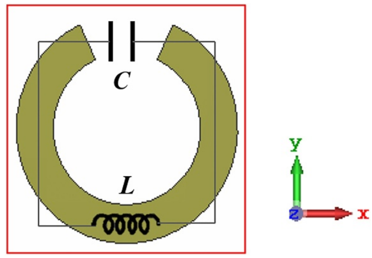

FIGURE 1 Equivalent circuit of a single split ring resonators (SRR) structure.

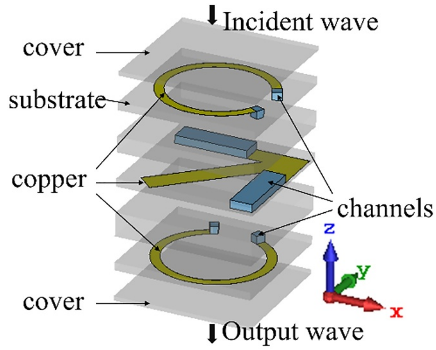

FIGURE 2 The topology of the proposed unit cell.

2.2 | Unit cell configuration

According to transmission matrix theory, the transmission unit cells with at least three metal layers can provide sufficient phase shift [15]. A fix transmission unit cell was proposed in the authors' previous work. Inspired by that work, a dynamic design is further proposed here.

Figure 2 shows the topology of the proposed unit cell. The structure consists of three conducting layers separated by dielectric substrates. The dielectric substrate is RO4003c with a permittivity of 3.55 and a loss tangent of 0.0027. Each of the three conducting layers incorporates a different resonator geometry. The arrow-shaped conducting layer has the capability to rotate the polarization direction by 90° [16]. It is orientated diagonally and placed on the middle layer. The SRR, on the upper and lower conducting layers, have the same size but different orientations.

Figure 3 shows the parameters of the unit cell. Table 1 gives the values of the parameters. By changing the length of the arrow arm along with the gaps of the split rings, the transmission behaviour of the unit cell can be changed. To do this, the channels, marked by blue, within the unit cell must be filled with liquid metal. These channels having a depth of 1.52 mm are made by cutting some slots into the dielectric substrates. They are placed beneath/above each conducting layer. In that case, the liquid metal can be in contact with the printed copper, thus the expected parameters (i.e. the arrow arm length and the gaps of the split rings) can be changed. Another two substrate layers are employed to form the uppermost and lowermost layers and act as covers to prevent the liquid metal from leaking out of the channels. The residual liquid could affect the results of antenna. In this work, to reduce the effects of residual fluids, the size of the channels are designed as small as possible. The smaller size of channel is, the lower wettability the liquid metal has, the less residue it will brings [17]. Also, the liquid metal is recycled and reused. Impurities such as dust and residual of the material that the channels (in previous designs where liquid metal is used) are made of will affect the antenna gain.

2.3 | Parametric study

To investigate into the sensitivity of the proposed unit cell, a parametric study was performed. The transmitarray unit cell is designed in an infinite array environment with Floquet ports excitation. The parametric study was undertaken within the full-wave simulation tool CST Microwave Studio 2019. Based on this study, the resonant frequency and transmission coefficient of the unit cell is primarily determined by the widths of split rings and arrow (including the width of liquid metal channels), respectively. Figure 4 shows that by increasing the width of split rings, the resonant frequency increases. By increasing the width of the arrow section, the transmission coefficient reduces. The transmission phase shift will not be significantly influenced. In this case, the insertion loss of the proposed unit cell could be further improved by tuning the widths of rings and arrow sections without affecting the phase shift range. However, better insertion loss requires narrower channels, which adds to the difficulty of injecting the liquid metal, in practice. So, we tried to make the channels wider whilst still providing an acceptable transmission coefficient.

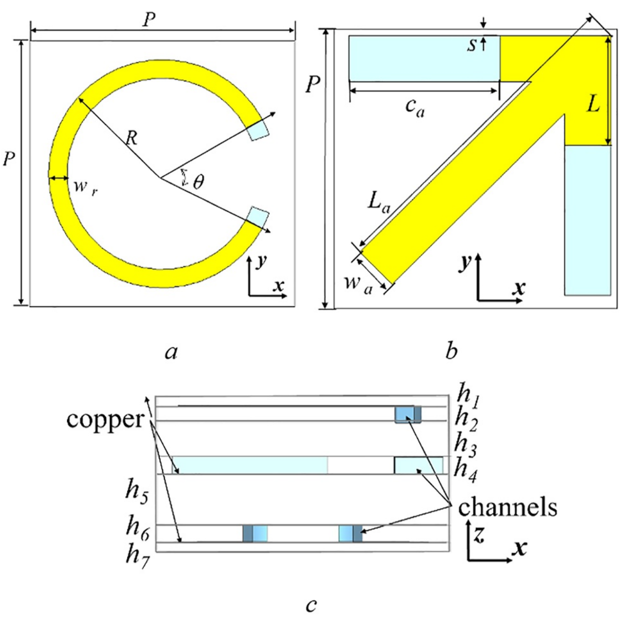

FIGURE 3 Top view of the (a) split ring layer, and (b) arrow layer. (c) Cross-sectional view of the unit cell in the xz-plane.

2.4 | Numerical results

The arrow arm length and the gaps within the split rings are changed by injecting liquid metal into the channels.

In turn, this tunes the transmission behaviour of the unit cell including the resonant frequencies and transmission phase. In this paper, a design having three reconfigurable states is proposed. Table 2 shows three reconfigurable states. When there is no liquid metal in all channels, the state is called State 1. When the gaps within the split rings on different conducting layers are full of liquid metal, the state is called State 2. When all channels are filled with liquid metal, the state is called State 3.

Figure 5a shows that the resonant frequency alters as the state alters. Figure 5b shows the corresponding transmission phase (∠S21) for the three states. When the state of unit cell is altered from State 1 to State 2, the transmission phase is changed from −57° to −147° at 3.3 GHz. When the state of unit cell is altered from State 2 to State 3, the transmission phase is changed from −147° to −377°. As a result, the total phase shifting range of the unit cell for the two tuning steps is around 330° at 3.3 GHz with 1.5 dB insertion loss. The unit cell has a 3-dB transmission bandwidth from 3.2 to 3.43 GHz.

3 | FABRICATION AND MEASUREMENT RESULTS

In this section, the fabrication consideration, actuation of liquid metal and measured results of the proposed reconfigurable unit cell are discussed.

3.1 | Fabrication and actuation

In the proposed design, the liquid metal based around an alloy consisting of 75% Gallium and 25% Indium (EGaIn) is employed. The conductivity of EGaIn is 3.4 × 106 S/m. Figure 6a shows the fabricated unassembled unit cell and its channels. Figure 6b shows the assembled unit cell inside an open-ended waveguide.

The waveguide method is an effective alternative to verify the performance of a unit cell [18, 19] and was selected to simplify manufacturing complexity, and to validate the simulation process. Figure 7a shows the measurement system. A horn antenna (ETS-Lindgren double-ridged horn 3115) was

TABLE 1 Optimized Dimensions of the Design Unit Cell (Unit: mm).

Parameter	P	R	w_r	w_a	s	c_a	L	L_a	θ	h_1	h_2	h_3	h_4	h_5	h_6	h_7
Value	26	11.16	1.8	4.2	0.68	13.9	10.1	26	57	0.813	1.52	3.04	1.52	4.56	1.52	0.813

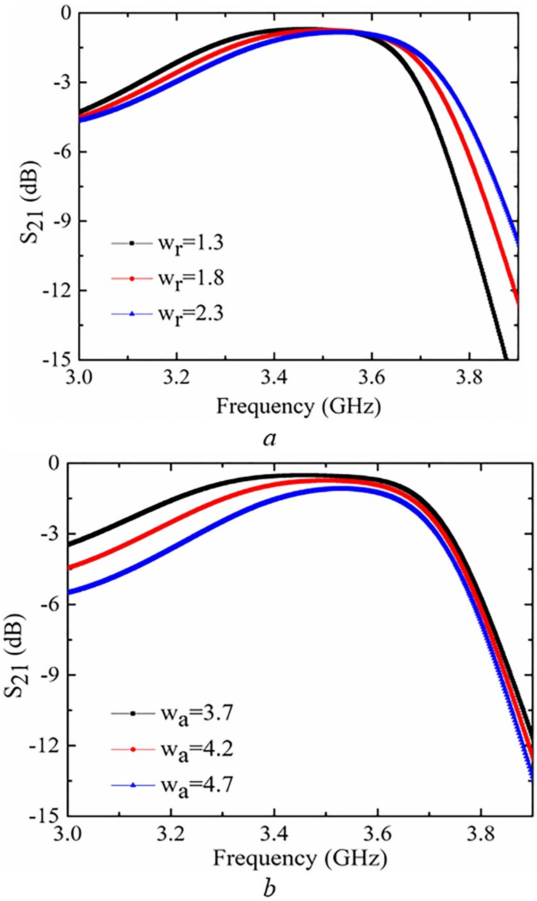

FIGURE 4 Parameter studies on (a) the width of rings and (b) the width of arrow.

TABLE 2 States of liquid metal.

State i	Double-rings channels	Arrow-head channels
1	No liquid metal	No liquid metal
2	Full of liquid metal	No liquid metal
3	Full of liquid metal	Full of liquid metal

used to receive the signal transmitted from the section of waveguide incorporating the unit cell. The horn was placed at a distance of 1m from the unit cell. The unit cell is excited by a standard WR284 waveguide (72 × 34 mm^2). By injecting liquid metal into the channels, it will be possible to alter the gaps within the split rings (θ) and the length of the arrow heads (Ca).

The liquid metal was injected manually using a syringe as shown in Figure 6c. This technique is widely used in the literature within proof-of-concept designs [20–31]. Inserting liquid metal manually into the channel when the structure is open and split into parts is not suitable for reconfiguration. This would be further improved by designing external inlets and outlets for the liquid to flow in and out. In this work, altering the method of actuation would have minimal effect on RF performance of the

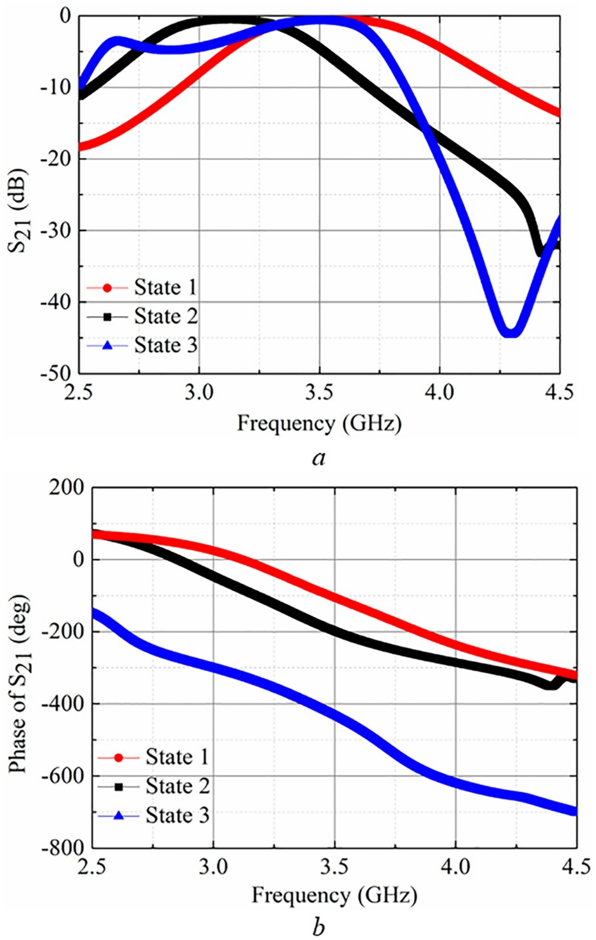

FIGURE 5 (a) Transmission amplitude and (b) transmission phase of the three states.

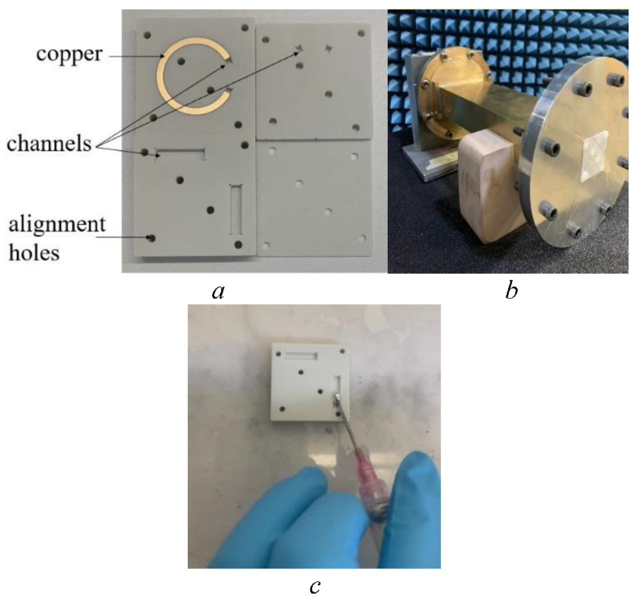

FIGURE 6 (a) The unassembled unit cell and its channels; (b) The unit cell inside at the end of waveguide; (c) The unit cell drained by a syringe.

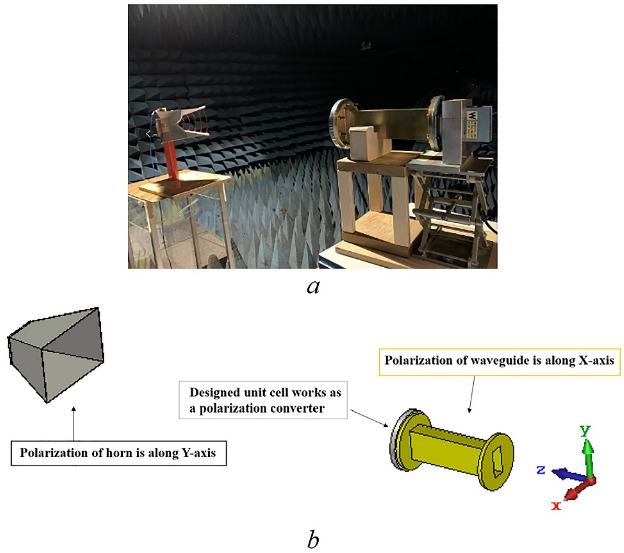

FIGURE 7 (a) The experimental setup of the open-ended waveguide; (b) The configuration of the simulation system which has the same settings as the measurement.

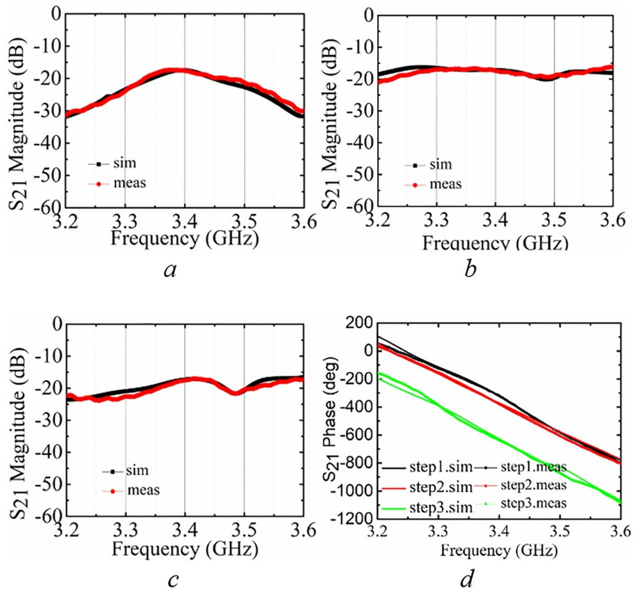

FIGURE 8 Simulated and measured transmission amplitude of the transmit-array unit cell under the measurement setup for (a) State1, (b) State2, and (c) State3. (d) Simulated and measured transmission phases of the States 1, 2, and 3 versus frequencies.

proposed antenna. Consequently, for this application, it is possible to control the liquid metal using a micropump [8] or electrochemically controlled capillary action [32].

3.2 | Measurement results

Due to the different environment between simulation and measurement, the fabricated unit cell cannot be compared directly with the unit cell simulated with periodic boundary conditions. Consequently, a system with the electrical boundary conditions as the measurement was simulated and compared with the measurement results. Figure 7b illustrates the simulation system; it shares the same configuration as the measurement system. By comparing the measured and simulated results of Figure 7, we could verify if the unit cell can be modelled correctly within the simulation environment. When the measured results agree well with simulated results, reasonable inferences can be drawn that the simulated results of the unit cell under periodic boundary conditions are reliable.

The proposed unit cell was measured and simulated in three reconfigurable states. Figure 8 depicts the comparison of the measured and simulated results. In Figure 8a, b and c, the transmission coefficients (S21) in three states are plotted against the frequency. The black curves represent the simulated results while the red curves represent the measured results of the proposed unit cell. In Figure 8d, the transmission phases in three states are plotted against the frequency. It can be concluded that the simulated results of the unit cell achieve good agreement with the measured results.

In Figure 8a, b and c, we notice that when the simulation shares the same configurations with the measurement, the simulated S21 is about 0.2 dB higher than the measured S21. The difference might be resulted from the misalignment, simulation and fabrication inaccuracy. Material loss might also contribute to the difference between measured and simulated results. The 0.2 dB difference is within the tolerance. It is worth noting that, by comparing the simulated results under periodic boundary conditions in Figure 5 with measured results in Figure 8, the simulated transmission coefficients have higher values than the measured results. Based on our measurement, the different results mainly come from the open space between the horn and the unit cell. The open space introduces free-space path loss, thus increases the attenuation of the transmission coefficient. Meanwhile, the mismatching of the cross-sectional dimensions of the unit cell and waveguide brings in attenuation. The agreement between the measured and simulated results under the same configurations validates the accuracy of our simulations of modelling the unit cell. We can infer that if the same boundary conditions is provided in the measurement, reasonable measured results can be achieved with a constant difference between simulated results. That is, the measured results should be 0.2 dB lower than the simulated results, under periodic boundary conditions.

In Figure 8d, the measured transmission phase shifts achieve good agreements with the simulated results. At 3.3 GHz, the measured results of phase shifting range is more than 300°. The simulated and measured phase shifting has a difference of 10°, which is only 3% of the phase shifting range. We consider the difference tolerable.

Based on the above analysis of measured and simulated results, we presume that at 3.3 GHz, our proposed transmit-array unit cell has a transmission coefficient of around −1.5 dB and can reasonably shift the phase by more than 300°.

Table 3 shows the comparison between the transmission properties of our proposed unit cell and other reconfigurable transmit-array unit cell reported in the literature. Our work improves the insertion loss of currently reconfigurable unit cell.

Ref.	Freq. (GHz)	Phase shifting range (deg)	Insertion loss (dB)	Control
[2]	5	400°	3.6	Varactors
[13]	8.8	360°	3	Liquid metal
[33]	15	0°/180°	2.58	PIN
[34]	13.5	0°/180°	1.8	PIN
Our work	3.3	330°	1.6	Liquid metal

TABLE 3 Comparison for unit cell performance.

Although three discrete states are shown in this paper, it is worth noting that if it is possible to inject liquid metal continuously into channels, the continuous phase shifting range of this unit cell can be obtained. To produce a fully controlled phase change, 0.2 mL volume of liquid metal needs to be injected.

4 | CONCLUSION

This paper presents a reconfigurable unit cell for use within transmitarray applications. The transmitarray unit cell is changed by employing liquid metal. The proposed unit cell incorporates three conducting layers with different geometries. Several channels are placed beneath/above the conducting layers. The transmission behaviour of the unit cell can be changed by injecting liquid metal into the channels. A 330° phase shift range with an S21 of ~ −1.5 dB at 3.3 GHz is obtained. The proposed unit cell exhibits 3 dB of insertion loss over a bandwidth ranging from 3.2 to 3.43 GHz. Compared with conventional electronically controlled unit cells, the proposed unit cell yields a good improvement in low insertion loss, large phase shift range, and reduced design complexity. The proposed prototype is fabricated and measured within an open-ended waveguide. The measured results agree well with the simulations and verify the effectiveness of the design. The proposed prototype is an attractive candidate for future transmitarray applications.

AUTHOR CONTRIBUTIONS

Zhishu Qu: Conceptualization, Methodology, Simulation, Performing the experiments, Writing - initial draft preparation. Yihua Zhou: Performing the experiments, Writing – review & editing. James R. Kelly: Supervision, conceptualization. Zhengpeng Wang: Manufacturing the antenna. Kenneth Lee Ford: Supervision. Yue Gao: Supervision.

ACKNOWLEDGEMENTS

This work was supported in part by a grant from The United Kingdom Engineering and Physical Sciences Research Council, EPSRC, under grant number: EP/P008402/1 and EP/P008402/2, in part by China Postdoctoral Science Foundation, under grant number: 2023TQ0076.

CONFLICT OF INTEREST STATEMENT

The authors declare that there is no conflict of interests, we do not have any possible conflicts of interest.

DATA AVAILABILITY STATEMENT

The data that support the findings of this study are available from the corresponding author upon reasonable request.

ORCID

Zhishu Qu https://orcid.org/0000-0002-6671-2647
Yihua Zhou https://orcid.org/0000-0003-1506-7964

REFERENCES

1. Lau, J.Y., Hum, S.V.: Analysis and characterization of a multipole reconfigurable transmitarray element. IEEE Trans. Antenn. Propag. 59(1), 70–79 (2010). https://doi.org/10.1109/tap.2010.2090456
2. Lau, J.Y., Hum, S.V.: A wideband reconfigurable transmitarray element. IEEE Trans. antennas propagation 60(3), 1303–1311 (2011). https://doi.org/10.1109/tap.2011.2180475
3. Clemente, A., et al.: 1-Bit reconfigurable unit cell based on PIN diodes for transmit-array applications in X-Band. IEEE Trans. Antenn. Propag. 60(5), 2260–2269 (2012). https://doi.org/10.1109/tap.2012.2189716
4. Di Palma, L., et al.: 1-bit reconfigurable unit cell for Ka-band transmitarrays. IEEE Antenn. Wireless Propag. Lett. 15, 560–563 (2015). https://doi.org/10.1109/lawp.2015.2458179
5. Schoenlinner, B., et al.: Switchable low-loss RF MEMS Ka-band frequency-selective surface. IEEE Trans. Microw. Theor. Tech. 52(11), 2474–2481 (2004). https://doi.org/10.1109/tmtt.2004.837148
6. Luo, Z., et al.: Active metasurface absorber for intensity- dependent surface-wave shielding. IEEE Trans. Antenn. Propag. 71(7), 5795–5804 (2023). https://doi.org/10.1109/tap.2023.3269160
7. Ma, X., et al.: A wideband 1-bit reconfigurable electromagnetic surface for monopulse radar applications. IEEE Trans. Antenn. Propag. 71(6), 5475–5480 (2023). https://doi.org/10.1109/tap.2023.3263204
8. Rodrigo, D., Jofre, L., Cetiner, B.A.: Circular beam-steering reconfigurable antenna with liquid metal parasitics. IEEE Trans. Antennas Propag. 60(4), 1796–1802 (2012). https://doi.org/10.1109/tap.2012.2186235
9. Bai, X., et al.: Wideband pattern-reconfigurable cone antenna employing liquid-metal reflectors. IEEE Antennas Wireless Propag. Lett. 17(5), 916–919 (2018). https://doi.org/10.1109/lawp.2018.2823301
10. Zhang, T., Chen, Y., Yang, S.: A wideband frequency- and polarization-reconfigurable liquid metal-based spiral antenna. IEEE Antenn. Wireless Propag. Lett. 21(7), 1477–1481 (2022). https://doi.org/10.1109/lawp.2022.3171845
11. Li, L., et al.: Polarization- and frequency-reconfigurable patch antenna using gravity-controlled liquid metal. IEEE Trans. Circuits Syst. Express Briefs 69(3), 1029–1033 (2022). https://doi.org/10.1109/tcsii.2021.3119040
12. Li, M., Behdad, N.: Fluidically tunable frequency selective/phase shifting surfaces for high-power microwave applications. IEEE Trans. Antenn. Propag. 60(6), 2748–2759 (2012). https://doi.org/10.1109/tap.2012.2194645
13. Erdil, E., et al.: Reconfigurable nested ring-split ring transmitarray unit cell employing the element rotation method by microfluidics. IEEE Trans. Antennas Propag. 63(3), 1163–1167 (2015). https://doi.org/10.1109/tap.2014.2387424

14. Zhu, W.M., et al.: Metamaterial tunable filter with liquid metal. In: 2013 IEEE 26th International Conference on Micro Electro Mechanical Systems (MEMS), pp. 725–728 (2013)
15. Qu, Z., Kelly, J.R., Gao, Y.: Analysis of the transmission performance limits for a multilayer transmitarray unit cell. IEEE Trans. Antennas Propag. 70(3), 2334–2339 (2022). https://doi.org/10.1109/tap.2021.3111162
16. Feng, P.Y., Qu, S.W.: 60-GHz 2D scan phased transmitarray with high gain and low profile. In: 2019 13th European Conference on Antennas and Propagation (EuCAP), pp. 1–4. IEEE (2019)
17. Dickey, M., et al.: Eutectic gallium-indium (EGaIn): a liquid metal alloy for the formation of stable structures in microchannels at room temperature. Adv. Funct. Mater. 18(18), 1097–1104 (2008). https://doi.org/10.1002/adfm.200701216
18. Di Palma, L., et al.: 1-Bit reconfigurable unit cell for ka-band transmitarrays. IEEE Antennas Wireless Propag. Lett. 15, 560–563 (2016). https://doi.org/10.1109/lawp.2015.2458179
19. Li, M., Behdad, N.: Fluidically tunable frequency selective/phase shifting surfaces for high-power microwave applications. IEEE Trans. Antennas Propag. 60(6), 2748–2759 (2012). https://doi.org/10.1109/tap.2012.2194645
20. Morishita, M., et al.: A liquid-metal monopole array with tunable frequency, gain, and beam steering. IEEE Antenn. Wireless Propag. Lett. 12(12), 1388–1391 (2013). https://doi.org/10.1109/lawp.2013.2286544
21. Mumcu, G., Dey, A., Palomo, T.: Frequency-agile bandpass filters using liquid metal tunable broadside coupled split ring resonators. IEEE Microw. Wireless Compon. Lett. 23(4), 187–189 (2013). https://doi.org/10.1109/lmwc.2013.2247750
22. Chen, W., et al.: Bendable and stretchable microfluidic liquid metal-based filter. IEEE Microw. Wireless Compon. Lett. 28(3), 203–205 (2018). https://doi.org/10.1109/lmwc.2018.2799382
23. Koo, C., et al.: Manipulating liquid metal droplets in microfluidic channels with minimized skin residues toward tunable RF applications. J. Microelectromech. Syst. 24(4), 1069–1076 (2014). https://doi.org/10.1109/jmems.2014.2381555
24. Rafi, M.A., Wiltshire, B.D., Zarifi, M.H.: Wideband tunable modified split ring resonator structure using liquid metal and 3-D printing. IEEE Microw. Wireless Compon. Lett. 30(5), 469–472 (2020). https://doi.org/10.1109/lmwc.2020.2980740
25. Ha, A., Kim, K.: Frequency tunable liquid metal planar inverted-F antenna. Electron. Lett. 52(2), 100–102 (2016). https://doi.org/10.1049/el.2015.3009
26. Watson, A.M., et al.: Physically reconfigurable RF liquid electronics via Laplace barriers. IEEE Trans. Microw. Theor. Tech. 67(12), 4881–4889 (2019). https://doi.org/10.1109/tmtt.2019.2950217
27. Vahabisani, N., Khan, S., Daneshmand, M.: Microfluidically reconfigurable rectangular waveguide filter using liquid metal posts. IEEE Microw. Wireless Compon. Lett. 26(10), 801–803 (2016). https://doi.org/10.1109/lmwc.2016.2605450
28. Song, L., et al.: Wideband frequency reconfigurable patch antenna with switchable slots based on liquid metal and 3-D printed microfluidics. IEEE Trans. Antenn. Propag. 67(5), 2886–2895 (2019). https://doi.org/10.1109/tap.2019.2902651
29. Kim, T., et al.: Micropatterning of liquid metal by dewetting. J. Microelectromech. Syst. 26(6), 1244–1247 (2017). https://doi.org/10.1109/jmems.2017.2723628
30. Low, J.H., Chee, P.S., Lim, E.H.: Deformable liquid metal patch antenna for air pressure detection. IEEE Sensor. J. 20(8), 3963–3970 (2019). https://doi.org/10.1109/jsen.2019.2961514
31. Bharambe, V.T., et al.: Multifunctional 3D printed antennas using liquid metal parasitics. IEEE Access 7, 134245–134255 (2019). https://doi.org/10.1109/access.2019.2942058
32. Wang, M., et al.: Pump free feedback control of a frequency reconfigurable liquid metal monopole. Proc. IEEE Int. Symp. Antennas Propag., 2223–2224 (2015). https://doi.org/10.1109/aps.2015.7305500
33. Xiao, Y., et al.: 1-Bit wideband reconfigurable transmitarray unit cell based on PIN diodes in ku-band. IEEE Antennas Wireless Propag. Lett. 20(10), 1908–1912 (2021). https://doi.org/10.1109/lawp.2021.3100494
34. Wang, Y., et al.: A novel 1 bit wide-angle beam scanning reconfigurable transmitarray antenna using an equivalent magnetic dipole element. IEEE Trans. Antennas Propag. 68(7), 5691–5695 (2020). https://doi.org/10.1109/tap.2020.2964954

How to cite this article: Qu, Z., et al.: A reconfigurable transmitarray unit cell employing liquid metal. IET Microw. Antennas Propag. 1–7 (2024). https://doi.org/10.1049/mia2.12518